



Warren, A. D., & Gates, P. J. (2020). Flavone as a novel matrix for the MALDI analysis of lanthanide and transition metal salts. *Journal of Mass Spectrometry*, 55(10), [e4609]. <https://doi.org/10.1002/jms.4609>

Peer reviewed version

Link to published version (if available):  
[10.1002/jms.4609](https://doi.org/10.1002/jms.4609)

[Link to publication record in Explore Bristol Research](#)  
PDF-document

This is the author accepted manuscript (AAM). The final published version (version of record) is available online via Wiley at <https://onlinelibrary.wiley.com/doi/abs/10.1002/jms.4609> . Please refer to any applicable terms of use of the publisher.

## University of Bristol - Explore Bristol Research

### General rights

This document is made available in accordance with publisher policies. Please cite only the published version using the reference above. Full terms of use are available:  
<http://www.bristol.ac.uk/red/research-policy/pure/user-guides/ebr-terms/>

Original paper

## **Flavone as a novel matrix for the MALDI analysis of lanthanide and transition metal salts**

Alexander D. Warren<sup>#</sup> and Paul J. Gates\*

### **Affiliations:**

School of Chemistry, University of Bristol, Cantock's Close, Bristol, BS8 1TS, United Kingdom.

# current address:

Interface Analysis Centre, School of Physics, University of Bristol, Tyndall Avenue, Bristol BS8 1TL, United Kingdom.

### **Corresponding Author**

Dr P. J. Gates

<paul.gates@bristol.ac.uk>

Tel: 44 (0)117 3317192

Fax: +44 (0)117 9251295

### **Keywords**

Maldi matrix, flavone, lanthanide

## **Abstract**

The mass spectral analysis of metal salts, especially lanthanide and transition metal salts can be challenging. Although getting information on the metal present is usually straightforward, obtaining information on the correct oxidation state and anion composition is challenging. Many ionisation techniques have some redox component to the ionisation process which commonly results in changing the oxidation state of the metal and the associated loss of ligand and anion information. We present here a simple method for negative ion matrix-assisted laser desorption/ionisation mass spectrometry using the non-acidic flavonoid flavone as a novel matrix. This results in reliable information on the oxidation state of the metal as spectra are dominated by anion adduct ions with very little (typically no) redox processes occurring.

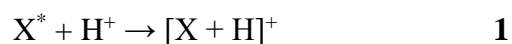
## **Introduction**

Matrix-assisted laser desorption/ionisation (MALDI) mass spectrometry (MS) is a well-established technique for the analysis of high molecular weight species, (synthetic polymers, proteins, peptides, polysaccharides etc.) but is always challenging for the analysis of low molecular weight (LMW) species [1]. Over the last 20 years, there has been considerable work to try to design methodologies for the successful analysis of LMW analytes.

Normally, the analysis of LMW analytes (e.g. small organics, metal salts, and complexes) is hindered by the presence of the matrix itself. MALDI matrices are typically LMW compounds themselves and as a result, ions due to their ionisation, fragmentation and clustering typically dominate the low-mass regions of spectra, sometimes to the extent that any signals due to the analyte are totally obscured or, in extreme cases, totally suppressed [1]. This very undesirable result, termed ‘analyte suppression’, leads to reduced spectral quality and even mistaken analyte identification. Figure 1 is the MALDI-MS spectrum of the flavanone hesperetin ( $M_w = 302$ ) using 2,5-dihydroxybenzoic acid (DHB) as the matrix. The spectrum is a typical example of analyte-suppression, where the identification of an unknown analyte would have been significantly hindered by the intense matrix signals.

A method for reducing the abundance of matrix related ions detected, and thus improve the applicability of MALDI for the analysis of LMW analytes, is by utilisation of the Matrix Suppression Effect (MSE) [2-4]. Key parameters that have effects on the level of the MSE

observed are the laser intensity and analyte-to-matrix ratio. This is primarily due to the competitive nature of the ionisation (see equations **1** to **3**) between matrix (X) and analyte (M).



Where the process shown in equation **3** is favoured compared to processes shown in equations **1** and **2**, successful MSE will occur, resulting in higher quality spectra. However, in most cases it is processes **1** and **2** that are occurring in competition.

Studies have been undertaken into the use of additives to enhance the MSE by reducing the number of protons available for reaction. This includes altering the pH of the system to make it more basic [4] or by introducing additives (A) to react with the excited matrix ions in the plume [5], deprotonating them and preventing them from being detected (see equation **4**).



Alternative methods for improving the application of MALDI-MS for the analysis of LMW analytes would be to find new matrices which either enhance analyte ionisation, or give very little signal themselves - there is considerable continuing research in this area:

Analysis of hydrocarbons either from synthetic sources or from natural sources like crude oils is largely limited to the analysis of the volatile fractions by techniques such as EI or APCI. The involatile components most always need desorption ionisation methods, but if the target analytes are also non-polar then MALDI is the only real technique available. There have been considerable successes in this area making use of reactive matrices like fullerenes intercalated with cobalt metal ions [6], silver nitrate doped ionic matrices [7] or ammonium exchanged zeolites [8]. Ionic matrices have also shown considerable successes in the investigation of counterfeit pharmaceuticals [9].

A recent study in the Czech Republic used aqueous solutions of the lithium salts of aromatic acids as matrices for the analysis of hydrocarbons and waxes [10]. Resultant spectra were almost totally devoid of matrix related ions in the positive ion mode which allowed the

successful detection of shorter chain hydrocarbons. The authors put this down to improved absorption of UV radiation and enhanced solubility of the matrices as well as efficient transfer of the lithium cation to the analytes in the gas-phase. This method has also been applied to a wider range of natural products [11].

Another study in China, used metal-phthalocyanines as matrices for the analysis of small molecules [12, 13]. This method showed high levels of success for the analysis of LMW acids through complexation of the analyte with the phthalocyanines. A more recent Chinese study employed graphene oxide as the matrix for *in situ* analysis of phospholipids by MALDI imaging [14]. This work clearly demonstrates about 2 orders of magnitude increase in signal-to-noise from the same sample when compared to DHB.

There have been several recent studies reporting on the use of flavonoids as MALDI matrices for both direct analysis and imaging studies [15-18]. The flavonoids quercetin and rutin were utilised in the analysis of both platinum and palladium complexes. These flavonoid matrices were found to be effective at low matrix concentrations yielding spectra with low levels of noise. Wang *et al* [18] tested a range of flavonoid aglycones as matrices for MALDI imaging of lipids in tissue samples and found that those with an OH group in the C3 or C5 position gave the best performance. The authors found also that quercetin along with morin were successful matrices.

One thing all these methodologies and new matrices have in common, is that they have limited application to the analysis of negatively charged analytes. During our own ongoing study into the utility of MALDI mass spectrometry for the analysis of low molecular weight (LMW) analytes [19], a large-scale comparison project was performed. During this project it was observed that when the flavonoid aglycone flavone (see figure 2) was analysed using several traditional matrices, only very weak flavone peaks were observed in the resulting spectra. Instead the spectra were almost completely dominated by matrix peaks – i.e. very high levels of analyte suppression was occurring (see figure 3). Interestingly, in negative ion mode, peaks were observed for all three traditional matrices studied. Typically, traditional matrices yield poor spectra in negative ion mode when analysed by LDI (i.e. without another matrix being present) so this finding is highly interesting as evidently their ionisation was being assisted in some way. From this it was deduced that flavone may be acting as a matrix and thus enhancing the ionisation of the ‘traditional matrices’ in the negative ion mode.

We believe that this novel behaviour exhibited by flavone sets it apart from the other flavonoid matrices (quercetin, rutin and morin would all appear to behave similarly to ‘traditional’ MALDI matrices with regard to the species observed [11-14]). Therefore, this paper presents a study of the possible matrix behaviour of flavone for negative ion MALDI-MS analysis. This study uses a range of pure heavy metal and lanthanide oxides and their salts as analytes to exemplify this behaviour. Analysis of this type of analyte is not straightforward by MS. Whereas ICP-MS gives reliable information about metal content and quantification from complex environmental and/or biological matrices, it provides little information about the context of the metal in the original sample – for example the original oxidation state of the metal, nature of any counter ions or whether or not it was present as an oxide. The methodology presented in this study, is a simple and effective way to obtain a reliable qualitative analysis of heavy metals and lanthanide salts using MALDI-MS. The results are compared to those obtained from a comparison study using a range of existing matrices (both ‘traditional’ organic acids and colloidal graphite) [19] for a range of pure analytes.

## **Experimental**

### *Instrumentation*

All mass analyses were performed on a 4700 Proteomics Analyzer (Applied Biosystems, Warrington, UK). This is a reflectron Time-of-Flight/Time-of-Flight (TOF/TOF) mass analyser, used in reflectron mode. All spectra were recorded at 1000 shots per spectrum (comprised of 8 sub-spectra, over a 5s run) at a resolution of approximately 25,000 FWHM. The laser used was a 200 Hz Nd/YAG at a wavelength of 355 nm. The laser beam diameter is 50  $\mu\text{m}$  with pulse energy of 12  $\mu\text{J}$  and pulse length of less than 500 ps. Calibration (better than 5ppm) was achieved using the 4700 Proteomics Analyzer Calibration Mixture (Applied Biosystems, Warrington, UK). Calibration accuracy and variation was checked externally using a mixture of PEG200/400.

### *Chemicals*

2,5 – Dihydroxybenzoic acid (DHB) was purchased from Fisher Scientific (Loughborough, U.K.). Flavone (F),  $\alpha$ -Cyano-4-hydroxycinnamic acid (CHCA), Sinapinic acid (SA) were all purchased from Sigma Aldrich (Gillingham, U.K.). Edelgraphit Graphite Aerosol Spray was purchased from the Graphite Trading Company (Halesowen, U.K.). All solvents used

throughout the study were HPLC gradient grade purchased from Fisher Scientific (Loughborough, U.K.).

Iron (II) Chloride, Lanthanum (III) Carbonate Hydrate, Neodymium (II) Iodide, Neodymium (III) trifluoromethanesulfonate, Ytterbium (III) acetate hydrate and Ytterbium (III) nitrate pentahydrate were all obtained from Sigma Aldrich (Gillingham, U.K.). Lanthanum (CPI international, Santa Rosa, California, USA), Uranium oxide (Spex CertiPrep, New Jersey, USA) and Neodymium and Samarium (Johnson Matthey, London, UK) were supplied as ICP standards in nitric acid solution and were assumed to be the corresponding nitrate salts at oxidation state (III). All analytes were used at a concentration of 125 ppm.

The organic matrices were prepared to a concentration of 5 mg/mL in methanol. The colloidal graphite matrix was prepared by spraying the aerosol can into a vial until approximately 1 mL of fluid collected at the bottom and then made up by adding 7 mL of water. [19] The matrices were mixed in a one-to-one ratio with the analyte solution prior to pipette deposition onto the target plate, so that co-crystallisation could occur.

## Results and discussion

During an investigation into the use of new matrices for the analysis of LMW analytes, the natural product flavone (see figure 2) was being analysed with a range of different matrices. It was immediately observed that flavone behaved differently to the other analytes. Figure 3 shows the MALDI-MS analysis of flavone using CHCA matrix as an example. Spectrum (a) is the positive ion mode spectrum, where the two most intense ions observed are the sodiated and potassiated ions of CHCA at  $m/z$  212 and 228 respectively. Alongside these are two very low intensity ions corresponding to the sodiated and potassiated ions of flavone at  $m/z$  245 and 261 respectively. There is also considerable noise in the spectrum in the range from  $m/z$  150 to 400. This is a typical positive ion mass spectrum. It becomes more interesting when the negative ion spectrum in figure 3(b) is considered. Here there are only two ions observed which are the deprotonated and decarboxylated ions of CHCA at  $m/z$  188 and 144 respectively - the spectrum is effectively devoid of any other ions. When performing negative ion MALDI with acidic matrices, you would expect to see the deprotonated ion of the matrix, but not to this level of intensity. This led the authors to consider that something different was happening here and that perhaps the ionisation of the matrix was being enhanced by the analyte.

A selection of traditional MALDI matrices (CHCA, DHB and SA) were subsequently run with flavone at matrix concentrations and the 'traditional' matrices at typical analyte concentrations (1mg/mL) to confirm the earlier observations of matrix activity enabling the ionisation of the 'traditional' matrices (see table 1 and figure S1 in SI). As can be seen from the data, this is indeed the case - with only readily identifiable ions of the 'traditional' matrices being yielded. This demonstrates that flavone is a more effective matrix than the 'traditional' matrices for negative ion analysis, as it can 'out-perform' them to ionise the traditional matrix in preference to itself being ionised. This was evident in the original observations where flavone was present at low concentrations as an analyte - when the 'traditional' matrix is used as the analyte and the concentrations are adjusted it becomes more apparent.

After this initial test, a systematic investigation of the use of flavone as a matrix (at typical matrix concentrations) for a range of metal salts was performed. The results were compared with the traditional matrices DHB and CHCA as well as the established but still relatively novel matrix colloidal graphite (CG) [19]. A summary of the results, detailing the analyses of a series of lanthanide nitrates (of the general formula  $\text{Ln}(\text{NO}_3)_3$ , where Ln represents the Lanthanide used) and the species observed across the range of matrices tested is given in table 2. Spectra are contained in the SI figures S2 to S13.

Typically the peaks observed in positive ion mode with DHB were intact cationised DHB peaks ( $[\text{M}+\text{H}]^+$ ,  $[\text{M}+\text{Na}]^+$  and/or  $[\text{M}+\text{K}]^+$ ) along with singly charged naked metal cations and unidentifiable matrix clusters. This is the typical behaviour expected for DHB [20]. In the negative ion mode DHB was more successful in generating an intact metal salt peak in approximately 50% of cases (usually by anion attachment, although the spectra were typically dominated by the deprotonated DHB peak  $[\text{M}-\text{H}]^-$ ). The peaks observed in positive ion mode with CHCA were almost entirely due to matrix cationised peaks, as well as matrix dehydration  $[\text{M}+\text{H}-\text{H}_2\text{O}]^+$  and decarboxylation  $[\text{M}+\text{H}-\text{CO}_2]^+$ . In many cases, there was also significant cluster ion formation. In the negative ion mode, the CHCA spectra were dominated by deprotonation and decarboxylation of the matrix. In a few cases a low intensity intact metal salt peak was also observed. These observations for DHB and CHCA clearly demonstrate how inapplicable traditional organic (acidic) matrices are for the detection of metal salts in MALDI-MS.



The use of colloidal graphite (CG) as a matrix for LMW MALDI has already been studied extensively by the authors research group [19]. In this study, the peaks observed in the positive ion mode with CG were dominated by the singly charged naked metal cations, cation oxides and carbides. This is useful in generating information about what metal is present, although it gives no information regarding the original oxidation state, nor which anion is present. In the negative ion mode the spectra contained a mixture of anion attached complexes (of the general formula  $[\text{Ln}(\text{NO}_3)_4]^-$ ), oxide complexes (of the general formula  $[\text{LnO}(\text{NO}_3)_3]^-$ ), metal/anion cluster ions (of the general formula  $[\text{Ln}_2(\text{NO}_3)_7]^-$ ) and anionic carbon clusters  $\text{C}_n^-$ . These results are a significant improvement on what is observed with the 'traditional' organic matrices, with the intact metal nitrate dominating the spectra in all cases. However, the presence of the oxides and larger anion/cation clusters confuses the results, making interpretation uncertain and potentially ambiguous. Despite this, a further beneficial point is that the metal is always observed in the correct oxidation state.

For the analyses performed in the positive ion mode with flavone, the results mirror those observed with the other organic matrices - the spectra are dominated by the cationated matrix and singly charged naked cations. Most of the analyses with flavone matrix in the negative ion mode yielded exceptionally clean and clear spectra, at very good signal-to-noise ratios. For the majority of the lanthanide nitrates analysed, the only significant peak in the spectra correlated to the counter ion adduct, with the occasional presence of an identifiable analyte cluster at higher masses (see figure 4 for typical spectra).

These results using flavone as a matrix were intriguing enough to merit further work, as it suggested a highly unusual and very useful matrix action. Figure 5 shows further examples of spectra obtained using flavone as the matrix for the analysis of a range of metal salts.

The trend for positive ion spectra yielding ions mostly corresponding to cationised flavone species (data not shown) was maintained for all the analytes studied, and as a result these analyses will not be discussed any further.

In the negative ion spectra, there was a range of results which will be discussed further. General trends are that the naked anion is usually observed when the instrument is set to scan the mass range including it. Unfortunately, such mass ranges were not included in all the examples shown in figure 5 - given the reproducibility of the behaviour over a wide range of samples the

authors feel it is safe to assume that this behaviour is ubiquitous. In many cases, cluster ions of sodium (and potassium) with the anion are also observed. In the case of Bismuth nitrate these are the base peak. Sodium is typically ubiquitous, and as such this is not surprising, in the same way that sodium cationation is common in positive mode. Some of the analyses generated the flavone anion at  $m/z$  222. This is probably the result of electron transfer from the metal into the delocalized  $\pi$ -system of flavone. The presence of this peak does not appear to have a detrimental effect on the quality of the spectra obtained.

- For the spectrum of Bismuth nitrate, as well as the general ions mentioned above, the second most intense ion is for  $[\text{Bi}(\text{NO}_3)_4]^-$  ( $m/z$  457) i.e. the nitrate adduct of the analyte, with the bismuth remaining in the correct oxidation state. The only other ion of interest is a cluster ion of flavone with sodium and nitrate ( $m/z$  306). This is the only incidence of such an ion in this study but was consistently observed with this analyte.
- In the analysis of cobalt nitrate, the base peak was  $[\text{Co}(\text{NO}_3)_3]^-$  ( $m/z$  245) i.e. the nitrate adduct of the analyte, with the cobalt remaining in the correct oxidation state. There is also a low intensity ion for a cobalt oxide nitrate ( $m/z$  199), with some unidentified cluster ions at higher  $m/z$ .
- In the analysis of iron chloride, the base peak was  $[\text{FeCl}_4]^-$  ( $m/z$  161) i.e. the chloride adduct of the analyte, with the iron remaining in the correct oxidation state. However, as well as the cluster ion at  $m/z$  289, there are also significant peaks for  $[\text{FeCl}_2]^-$  ( $m/z$  126) and  $[\text{FeCl}_4]^-$  ( $m/z$  198) which suggest a certain degree of disproportionation is occurring during ionisation. This is perhaps not unexpected for iron as the redox potentials are all quite low.
- In the analysis of lanthanum carbonate, the base peak was  $[\text{La}(\text{CO}_3)_2]^-$  ( $m/z$  259) i.e. a fragment of the analyte with the lanthanum remaining in the correct oxidation state. This was the only time this kind of fragmentation was observed (but it should be noted that lanthanum carbonate was the only bimetallic complex included in this study). There is also a weak peak for  $\text{LaCl}_4^-$  ( $m/z$  279) and a lot of low-mass ions which were not identified. This was considered the worst result in this study; despite this the correct metal oxidation state and anion are still dominating the spectrum.
- In the analysis of neodymium iodide, the base peak was  $\text{NdI}_4^-$  ( $m/z$  650) i.e. the iodide adduct of the analyte with the neodymium remaining in the correct oxidation state. There is another unidentified neodymium peak at  $m/z$  585 and a few low intensity ions at lower mass.

- For the analysis of neodymium triflate, the base peak was  $[\text{Nd}(\text{CF}_3\text{O}_2\text{S})_4]^-$  ( $m/z$  740) i.e. the triflate adduct of the analyte with the neodymium remaining in the correct oxidation state. The only other significant ion was for  $[\text{Nd}(\text{CF}_3\text{O}_2\text{S})_3\text{F}]^-$  ( $m/z$  610) which is the fluoride adduct of the analyte. There is also the expected peak for the triflate anion at  $m/z$  149.
- For the analysis of rubidium nitrate, the base peak was  $[\text{Rb}(\text{NO}_3)]^-$  ( $m/z$  147) and the second most intense peak was for  $[\text{Rb}(\text{NO}_3)_2]^-$  ( $m/z$  209) i.e. the nitrate adduct of the analyte with the rubidium remaining in the correct oxidation state. This is one of the only occurrences where redox processes were observed using flavone as a matrix.
- The analysis of strontium nitrate gave the most complex spectrum with a wide number of unidentified peaks. The base peak was for  $[\text{SrNO}_2(\text{NO}_3)_2]^-$  ( $m/z$  242) and the nitrate adduct peak of the analyte was also observed at  $m/z$  274. This, however, is a complex spectrum and doubts have been raised as to the purity of the analyte. In the strontium containing peaks, the correct oxidation state is observed.
- The spectrum of uranium oxide nitrate only contained a single peak at  $m/z$  456 (for  $[\text{UO}_2(\text{NO}_3)_3]^-$ ). This is the nitrate adduct of the analyte with the uranium remaining in the correct oxidation state.
- With Ytterbium acetate, the base peak was for  $[\text{Yb}(\text{Ac})_3\text{Cl}]^-$  ( $m/z$  422) i.e. the chloride adduct of the analyte with the ytterbium remaining in the correct oxidation state.

Clearly, the analysis of metal salts remains problematic, but these results represent a quick and easy methodology to obtain information about the anion, the cation and the correct oxidation state. Redox processes (common in electrospray ionisation, for example [21]) were rarely observed in the negative ion mode with flavone as the matrix such that spectra were most often totally dominated by the anion adduct species (with lower intensity ions for the naked anion, sodium-anion clusters and the flavone anion). In some cases, spectra were complicated by additional unidentified peaks, alternative anion adducts ( $\text{F}^-$ ,  $\text{Cl}^-$  or  $\text{NO}_2^-$ ) and the creation of oxides. The reason why some analytes preferentially ionise via oxide formation or with different anions is unknown at this time but would benefit from further study.

Following the success of flavone as a general matrix to obtain useful spectra in MALDI analyses of metal salts, an additional experiment was undertaken to probe the homogeneity of pipette deposited flavone (see figure 6). Flavone generated very high quality, high intensity single spot images. The resulting images were very clear, with negligible background noise

from the plate - given the very low noise encountered during the use of flavone as a matrix in standard MALDI, this is not surprising. The images have large regions of brighter colours, corresponding to higher signal intensities. Whether these are abnormally large 'sweet spots' is unclear, however in many cases they occupy a significant region of the sample spot and as such defy the typical definition of a 'sweet spot' [20]. This makes flavone amenable to automated analysis as issues arising from 'sweet spots' (common with many traditional organic matrices) appear minimal. The analyte signal on the spots is evenly distributed, with a high preference for the sample plate surface rather than sitting in the spot perimeter-well - commonly observed for traditional matrices such as DHB.

## Conclusions

Comparing quercetin, rutin and flavone; they all share the same basic 2-phenylchromen-4-one flavonoid carbon skeleton; but that there are significant differences in terms of functionality – quercetin and rutin have hydroxyl groups with acidic protons, whilst flavone does not. As a result, quercetin and rutin can be considered as traditional organic matrices that add to the arsenal of successful matrices for positive mode analyses. Flavone is thought to exhibit a unique matrix behaviour - it appears to enhance ionisation of the analyte in negative ion mode without itself being ionised - hence we present this as a new technique in the MALDI family. In a few spectra the flavone anion is observed at  $m/z$  222 at low intensity. This is not detrimental to the success of the analysis and can be ignored.

The routine analysis of heavy metal and lanthanide oxides and salts is not straightforward by MS. ICP-MS gives reliable information about metal content from complex environmental and/or biological matrices, but provides little information about the context of the metal in original sample – i.e. the original oxidation state of the metal, the counter ion or whether or not it was present as the oxide. The methodology presented in this study, is a simple and effective way to obtain a reliable qualitative analysis of heavy metals and lanthanide salts using MALDI-MS with the readily available and cheap new matrix flavone. It requires no additional instrumentation, complex sample preparation, user expertise or knowledge beyond that required for a standard MALDI-MS experiment. The results show that by using this simple methodology, we can correctly identify the anion, ligand, and correct original oxidation state of the metal. The authors believe that this new methodology can easily be adopted by MS facilities to broaden the range of analytes that can be reliably analysed.

As flavone is an entirely new matrix, there is a vast scope for further development. The work thus far has demonstrated a high success rate for analysis of a range of metal salts, including species of differing oxidation state and counter ions. Further expansion of this library would probe the application of the technique to the analysis of a wider range of inorganic salts and possibly more challenging inorganic and organometallic complexes.

### **Acknowledgments**

The authors acknowledge the University of Bristol, School of Chemistry Mass Spectrometry Facility for access to instrumentation and Dr Christopher Arthur for useful discussions throughout this project.

## References:

- [1] L.H. Cohen, A.I. Gusev; Small molecule analysis by MALDI mass spectrometry. *Anal. Bioanal. Chem.*, 2002, 373: 571-586.
- [2] G. McCombie, R. Knochenmuss; Small-Molecule MALDI using the matrix suppression effect to reduce or eliminate matrix background interferences. *Anal. Chem.*, 2004, 76: 4990-4997.
- [3] T.W.D Chan, A.W. Colburn, P.J. Derrick; Matrix-assisted UV laser desorption. Suppression of the matrix peaks. *Org. Mass Spectrom.*, 1991, 26: 342-344.
- [4] I.P. Smirnov, X. Zhu, T. Taylor, Y. Huang, P. Ross, I. A. Papayanopoulos, S. A. Martin, D.J. Pappin; Suppression of  $\alpha$ -Cyano-4-hydroxycinnamic acid matrix clusters and reduction of chemical noise in MALDI-TOF mass spectrometry. *Anal. Chem.*; 2004, 76: 2958-2965.
- [5] Z. Guo, Q.C. Zhang, H.F. Zou, B.C. Guo, J.Y. Ni; A method for the analysis of low-mass molecules by MALDI-TOF mass spectrometry. *Anal. Chem.*, 2002, 74: 1637-1641.
- [6] W.E. Wallace; Reactive MALDI mass spectrometry: application to high mass alkanes and polyethylene. *Chem. Commun.*, 2007, 4525–4527.
- [7] E. Lorente, C. Berruero, A.A. Herod, M. Millan, R. Kandiyoti; The detection of high-mass aliphatics in petroleum by matrix-assisted laser desorption/ionisation mass spectrometry. *Rapid Commun. Mass Spectrom.*, 2012, 26: 1581–1590.
- [8] M. Yang, K. Hashimoto, T. Fujino; Silver nanoparticles loaded on ammonium exchanged zeolite as matrix for MALDI-TOF-MS analysis of short-chain n-alkanes. *Chem. Phys. Lett.*, 2018, 706: 525–532.
- [9] J.L. Bronzel Jr, C.D.F. Milagre, H.M.S. Milagre; Analysis of low molecular weight compounds using MALDI- and LDI-TOF-MS: Direct detection of active pharmaceutical ingredients in different formulations. *J. Mass Spectrom.*, 2017, 52: 752–758.
- [10] P. Horká, V. Vrkoslav, R. Hanus, K. Pecková, J. Cvačková; New MALDI matrices based on lithium salts for the analysis of hydrocarbons and wax esters. *J. Mass Spectrom.*, 2014, 49: 628–638.

- [11] D.B. Silva, N.P. Lopes; MALDI-MS of flavonoids: a systematic investigation of ionization and in-source dissociation mechanisms. *J. Mass Spectrom.* 2015, 50: 182-190.
- [12] S. Zhang, Y. Chen, J.A. Liu, S.X. Xiong, G.H. Wang, J. Chen, G. Q. Yang; New matrix of MALDI-TOF MS for analysis of small molecules. *Chin. Chem. Let.* 2009, 20: 1495-1497.
- [13] S. Zhang, J. Liu, Y. Chen, S. Xiong, G. Wang, J. Chen, G. Yang; A novel strategy for MALDI-TOF MS analysis of small molecules. *J. Am. Soc. Mass Spectrom.* 2010, 21: 154-160.
- [14] Z. Wang<sup>1</sup>, Y. Cai, Y. Wang, X. Zhou, Y. Zhang, H. Lu; Improved MALDI imaging MS analysis of phospholipids using graphene oxide as new matrix. *Sci. Rep.* 2017, 7: no. 44466.
- [15] M. Petković, A. Vujčić, J. Schiller, Z. Bugarčić, J. Savić, V. Vasić; Application of flavonoids - quercetin and rutin - as new matrices for matrix-assisted laser desorption/ionization time-of-flight mass spectrometric analysis of Pt(II) and Pd(II) complexes. *Rapid Commun Mass Spectrom.* 2009, 23:1467-1475.
- [16] M. Petković, B. Petrović, J. Savić, Ž. D. Bugarčić, J. Dimitrić-Marković, T. Momić, V. Vasić; Flavonoids as matrices for MALDI-TOF mass spectrometric analysis of transition metal complexes. *Int. J. Mass Spectrom.* 2010, 290: 39-46
- [17] B. Damnjanović, B. Petrović, J. Dimitrić-Marković & M. Petković; Comparison of MALDI-TOF mass spectra of [PdCl(dien)]Cl and [Ru(en)<sub>2</sub>Cl<sub>2</sub>]Cl acquired with different matrices. *J. Serb. Chem. Soc.* 2011, 76: 1687-1701.
- [18] X. Wang, J. Han, A. Chou, J. Yang, J. Pan, & C. H. Borchers; Hydroxyflavones as a new family of matrices for MALDI tissue imaging. *Anal. Chem.* 2013, 85: 7566-7573.
- [19] A.D. Warren, U. Conway, C.J. Arthur, P. J. Gates; Investigation of colloidal graphite as a matrix for matrix-assisted laser desorption/ionization mass spectrometry of low molecular weight analytes; *J. Mass Spectrom.*, 2016, 51: 491-503.
- [20] S.L. Luxembourg, L.A. McDonnell, M.C. Duursma, X. Guo, R.M.A. Heeren; Effect of local matrix crystal variations in matrix-assisted ionization techniques for mass spectrometry; *Anal. Chem.*, 2003, 75, 2333-2341.

[21] G.J. van Berkel, V. Kertesz; Using the electrochemistry of the electrospray ion source; *Anal. Chem.*, 2007, 79, 5510-5520.



**Table 1.** Ions observed in the analysis of the 'traditional' matrices (DHB, CHCA and SA) as analytes and flavone (F) as the matrix.

Analyte	Ions Observed	
	Positive Mode	Negative Mode
2,5 – Dihydroxybenzoic acid (DHB)	[DHB+Na] <sup>+</sup> [DHB+K] <sup>+</sup>	[DHB-H] <sup>-</sup> [DHB-H-CO <sub>2</sub> ] <sup>-</sup>
α-Cyano-4-hydroxycinnamic acid (CHCA)	[CHCA+Na] <sup>+</sup> [CHCA+K] <sup>+</sup> [F+Na] <sup>+</sup> [F+K] <sup>+</sup>	[CHCA-H] <sup>-</sup> [CHCA-H-CO <sub>2</sub> ] <sup>-</sup>
Sinapinic acid (SA)	[SA+H] <sup>+</sup> [SA+H-H <sub>2</sub> O] <sup>+</sup> clusters	[SA-H] <sup>-</sup> [SA-H-H <sub>2</sub> O] <sup>-</sup>

**Table 2:** Table showing the comparison of the peaks observed in the MALDI analysis of a range of Lanthanide nitrates as the analytes with a range of matrices (indicated by X in the table). See SI figures S2-13 for all spectra. Base peak is indicated by bold red.

Analyte	DHB		CHCA		Colloidal Graphite		Flavone	
	Positive	Negative	Positive	Negative	Positive	Negative	Positive	Negative
La(NO <sub>3</sub> ) <sub>3</sub>	<b>[X+H]<sup>+</sup></b> [X+Na] <sup>+</sup> [X+K] <sup>+</sup> clusters	[X-H] <sup>-</sup> <b>[La(NO<sub>3</sub>)<sub>4</sub>]<sup>-</sup></b> unknown peaks	[X+H-CO <sub>2</sub> ] <sup>+</sup> <b>[X+H-H<sub>2</sub>O]<sup>+</sup></b> [X+H] <sup>+</sup> [X+Na] <sup>+</sup>	<b>[X-H]<sup>-</sup></b> [X-H-CO <sub>2</sub> ] <sup>-</sup> [La(NO <sub>3</sub> ) <sub>4</sub> ] <sup>-</sup>	La <sup>+</sup> <b>LaO<sup>+</sup></b> LaC <sub>n</sub> <sup>+</sup>	C <sub>n</sub> <sup>-</sup> <b>[La(NO<sub>3</sub>)<sub>4</sub>]<sup>-</sup></b> [La <sub>2</sub> (NO <sub>3</sub> ) <sub>7</sub> ] <sup>-</sup>	<b>La<sup>+</sup></b> [X+H] <sup>+</sup> [X+Na] <sup>+</sup> [X+K] <sup>+</sup> clusters	<b>[La(NO<sub>3</sub>)<sub>4</sub>]<sup>-</sup></b> [La <sub>2</sub> (NO <sub>3</sub> ) <sub>7</sub> ] <sup>-</sup>
Ce(NO <sub>3</sub> ) <sub>3</sub>	<b>Ce<sup>+</sup></b> [X+Na] <sup>+</sup> [X+K] <sup>+</sup>	<b>[X-H]<sup>-</sup></b> [Ce(NO <sub>3</sub> ) <sub>4</sub> ] <sup>-</sup> clusters	<b>[X+H-H<sub>2</sub>O]<sup>+</sup></b> [X+H] <sup>+</sup> [X+Na] <sup>+</sup> clusters	<b>[X-H]<sup>-</sup></b> [X-H-CO <sub>2</sub> ] <sup>-</sup>	Ce <sup>+</sup> <b>CeO<sup>+</sup></b> CeC <sub>n</sub> <sup>+</sup>	[CeO <sub>2</sub> (NO <sub>3</sub> ) <sub>2</sub> ] <sup>-</sup> <b>[CeO(NO<sub>3</sub>)<sub>3</sub>]<sup>-</sup></b> [Ce(NO <sub>3</sub> ) <sub>4</sub> ] <sup>-</sup>	Ce <sup>+</sup> [X+H] <sup>+</sup> <b>[X+Na]<sup>+</sup></b> [X+K] <sup>+</sup> clusters	[CeO(NO <sub>3</sub> ) <sub>3</sub> ] <sup>-</sup> <b>[Ce(NO<sub>3</sub>)<sub>4</sub>]<sup>-</sup></b> [Ce <sub>2</sub> (NO <sub>3</sub> ) <sub>7</sub> ] <sup>-</sup>
Nd(NO <sub>3</sub> ) <sub>3</sub>	Nd <sup>+</sup> <b>NdO<sup>+</sup></b> clusters	<b>NO<sub>2</sub><sup>-</sup></b> NO <sub>3</sub> <sup>-</sup> [X-H] <sup>-</sup>	[X+H-CO <sub>2</sub> ] <sup>+</sup> <b>[X+H-H<sub>2</sub>O]<sup>+</sup></b> [X+H] <sup>+</sup> [X+Na] <sup>+</sup> [2X+H] <sup>+</sup> clusters	<b>[X-H]<sup>-</sup></b> [X-H-CO <sub>2</sub> ] <sup>-</sup>	Nd <sup>+</sup> <b>NdO<sup>+</sup></b> clusters	C <sub>n</sub> <sup>-</sup> [NdO(NO <sub>3</sub> ) <sub>3</sub> ] <sup>-</sup> <b>[Nd(NO<sub>3</sub>)<sub>4</sub>]<sup>-</sup></b>	Nd <sup>+</sup> NdO <sup>+</sup> [X+H] <sup>+</sup> [X+Na] <sup>+</sup> <b>[X+K]<sup>+</sup></b> clusters	<b>[Nd(NO<sub>3</sub>)<sub>4</sub>]<sup>-</sup></b> [Nd <sub>2</sub> (NO <sub>3</sub> ) <sub>7</sub> ] <sup>-</sup>
Sm(NO <sub>3</sub> ) <sub>3</sub>	<b>Sm<sup>+</sup></b> SmO <sup>+</sup> clusters	<b>[X-H]<sup>-</sup></b> [Sm(NO <sub>3</sub> ) <sub>4</sub> ] <sup>-</sup> clusters	<b>[X+H-H<sub>2</sub>O]<sup>+</sup></b> [X+H] <sup>+</sup> [X+Na] <sup>+</sup> clusters	<b>[X-H]<sup>-</sup></b> [X-H-CO <sub>2</sub> ] <sup>-</sup>	<b>Sm<sup>+</sup></b> SmOH <sup>+</sup>	C <sub>n</sub> <sup>-</sup> [SmO(NO <sub>3</sub> ) <sub>3</sub> ] <sup>-</sup> <b>[Sm(NO<sub>3</sub>)<sub>4</sub>]<sup>-</sup></b>	[X+H] <sup>+</sup> <b>clusters</b>	<b>[Sm(NO<sub>3</sub>)<sub>4</sub>]<sup>-</sup></b> [Sm <sub>2</sub> (NO <sub>3</sub> ) <sub>7</sub> ] <sup>-</sup>
Gd(NO <sub>3</sub> ) <sub>3</sub>	[X+Na] <sup>+</sup> <b>[X+K]<sup>+</sup></b> clusters	<b>[X-H]<sup>-</sup></b>	[X+H-H <sub>2</sub> O] <sup>+</sup> [X+H] <sup>+</sup> <b>[X+Na]<sup>+</sup></b> [X+K] <sup>+</sup> clusters	<b>[X-H]<sup>-</sup></b> [X-H-CO <sub>2</sub> ] <sup>-</sup>	Gd <sup>+</sup> <b>GdO<sup>+</sup></b> clusters	[GdO(NO <sub>3</sub> ) <sub>3</sub> ] <sup>-</sup> <b>[Gd(NO<sub>3</sub>)<sub>4</sub>]<sup>-</sup></b>	[X+H] <sup>+</sup> <b>[X+Na]<sup>+</sup></b> [X+K] <sup>+</sup> clusters	<b>[Gd(NO<sub>3</sub>)<sub>4</sub>]<sup>-</sup></b> [Gd <sub>2</sub> (NO <sub>3</sub> ) <sub>7</sub> ] <sup>-</sup>
Yb(NO <sub>3</sub> ) <sub>3</sub>	<b>Yb<sup>+</sup></b> YbO <sup>+</sup> clusters	[X-H] <sup>-</sup>	[X+H-CO <sub>2</sub> ] <sup>+</sup> [X+H-H <sub>2</sub> O] <sup>+</sup> [X+H] <sup>+</sup> <b>[X+Na]<sup>+</sup></b> clusters	<b>[X-H]<sup>-</sup></b> [X-H-CO <sub>2</sub> ] <sup>-</sup> [Yb(NO <sub>3</sub> ) <sub>4</sub> ] <sup>-</sup>	<b>Yb<sup>+</sup></b> YbO <sup>+</sup> clusters	C <sub>n</sub> <sup>-</sup> <b>[Yb(NO<sub>3</sub>)<sub>4</sub>]<sup>-</sup></b>	<b>[X+H]<sup>+</sup></b> [X+Na] <sup>+</sup> [X+K] <sup>+</sup>	<b>[Yb(NO<sub>3</sub>)<sub>4</sub>]<sup>-</sup></b>

## Figure captions:

**Figure 1:** Spectrum obtained from the positive ion MALDI-MS analyses of hesperetin (*M* on the spectrum) using the traditional organic matrix DHB (*X* on the spectrum).

**Figure 2:** The structure of flavone (2-Phenyl-4-H-1-benzopyran-4-one).

**Figure 3:** Spectra obtained from the MALDI-MS analyses of flavone (*M*<sub>w</sub> 222) using CHCA (*M*<sub>w</sub> 189) as the matrix. Spectrum (a) is positive ion mode and (b) is negative ion mode.

**Figure 4.** The negative ion mode MALDI analysis of (a)  $\text{La}(\text{NO}_3)_3$  and (b)  $\text{Gd}(\text{NO}_3)_3$  using flavone as the matrix.

**Figure 5.** Spectra obtained from the negative ion mode analysis of a range of analytes using Flavone as the matrix. (a) Bismuth nitrate  $\text{Bi}(\text{NO}_3)_3$ , *M*<sub>w</sub>=395, (b) Cobalt nitrate  $\text{Co}(\text{NO}_3)_2$ , *M*<sub>w</sub>=183, (c) Iron chloride  $\text{FeCl}_3$ , *M*<sub>w</sub>=161 (d) Lanthanum carbonate  $\text{La}_2(\text{CO}_3)_3$ , *M*<sub>w</sub>=458, (e) Neodymium iodide  $\text{NdI}_3$ , *M*<sub>w</sub>=523, (f) Neodymium triflate  $\text{Nd}(\text{CF}_3\text{SO}_3)_3$  (g) Rubidium nitrate  $\text{Rb}(\text{NO}_3)$ , *M*<sub>w</sub>=147, (h) Strontium nitrate  $\text{Sr}(\text{NO}_3)_2$ , *M*<sub>w</sub>=212 (i) Uranium oxide nitrate  $\text{UO}_2(\text{NO}_3)_2$ , *M*<sub>w</sub>=394 and (j) Ytterbium acetate  $\text{Yb}(\text{C}_2\text{H}_3\text{O}_2)_3$ , *M*<sub>w</sub>=351.

**Figure 6:** Single spot images and camera photos (of the same spot) of (a) gadolinium nitrate imaged at *m/z* 406 (for the nitrate anion adduct:  $[\text{Gd}(\text{NO}_3)_4]^-$ ), (b) ytterbium nitrate imaged at *m/z* 422 (for the nitrate anion adduct:  $[\text{Yb}(\text{NO}_3)_4]^-$ ). Figure (c) shows the camera photo of the gadolinium nitrate spot and (d) is the camera photo of ytterbium nitrate spot. No filtering has been applied to these images. The colour coding in the images follows a 'heat map' principle with brighter tones (yellows, oranges, and reds) corresponding to stronger signals. Any signal coloured blue or brighter is considered a meaningful measurement.